Numerische Mathematik Manuscript-Nr.
(will be inserted by hand later)

A Finite-Element Capacitance Matrix Method for Exterior Helmholtz Problems

Oliver G. Ernst

Institut für Angewandte Mathematik II
TU Bergakademie Freiberg
09596 Freiberg, Germany

April 4, 1995

Summary. We introduce an algorithm for the efficient numerical solution of exterior boundary value problems for the Helmholtz equation. The problem is reformulated as an equivalent one on a bounded domain using an exact non-local boundary condition on a circular artificial boundary. An FFT-based fast Helmholtz solver is then derived for a finite-element discretization on an annular domain. The exterior problem for domains of general shape are treated using an imbedding or capacitance matrix method. The imbedding is achieved in such a way that the resulting capacitance matrix has a favorable spectral distribution leading to mesh independent convergence rates when Krylov subspace methods are used to solve the capacitance matrix equation.

Subject Classifications: 65N10, 65F30

1. Introduction

Capacitance matrix methods are numerical techniques aimed at bringing to bear the efficiency of fast elliptic solvers (cf. [6, 22]) on elliptic boundary value problems to which these fast solvers would otherwise not be applicable because the underlying problem is not separable. Fast elliptic solvers can be viewed as algorithms which efficiently apply a discrete Green's function belonging to a separable differential operator and domain to a grid function. The capacitance matrix method uses the discrete Green's function belonging to a separable domain containing the domain on which the problem is to be solved; for this reason, these techniques are also known as imbedding methods. The capacitance matrix then plays a role analogous to the integral operator whose kernel is the free-space Green's function (or some other fundamental solution belonging to the operator under consideration) when the integral equation method is used to solve the same elliptic boundary value problem.

Capacitance matrix methods are nearly as old as the fast elliptic solvers on which they are based. The first papers describing such techniques [14, 15, 7] appeared in the early seventies and treated discrete problems for Poisson's equation on bounded, non-separable domains. While these papers focused primarily on the matrix-theoretic aspects of the discrete problems, a series of papers by O. Widlund and his co-workers (cf. [10, 21, 4]) made use of the properties of the underlying continuous operators in order to design faster and more stable capacitance matrix algorithms for a large class of boundary value problems for self-adjoint, positive-definite operators. It was here also that the connection with the method of integral equations was explored. A brief history of capacitance matrix algorithms can be found in the author's dissertation [11], from which this paper is an excerpt.

We have developed an iterative finite-element capacitance matrix method for exterior boundary value problems for the Helmholtz equation. In extending capacitance matrix methods to this problem class, two difficulties must be overcome: the first is that the Helmholtz operator is generally indefinite and hence the sesquilinear form belonging to the corresponding variational problem is not coercive and thus the usual approach using the Lax-Milgram lemma to show existence and uniqueness cannot be used. The other is the fact that the exterior problem is posed on an unbounded domain and that the solution must satisfy an asymptotic boundary condition is needed in order for the solution of the exterior problem to be unique.

This paper is organized as follows. In Section 2, we state the problem and introduce an equivalent reformulation on a bounded domain suitable for discretization using the Dirichlet-to-Neumann (DtN) boundary condition (cf.[20, 16]), an exact non-local boundary condition on a circular artificial boundary. We then introduce the corresponding variational formulation and show that this problem has a unique solution following an idea of Masmoudi [20]. The finite element discretization is introduced in Section 3, where we show that the resulting finite dimensional problem has a unique solution as well. Section 4 introduces a fast Helmholtz solver on a separable domain, in this case an annulus, which also takes into account the DtN boundary condition. An iterative capacitance matrix algorithm based on this fast solver is then introduced in Section 5, where we also give a formal argument indicating that the convergence rate of the iteration is mesh independent. These considerations are supported by numerical results reported in Section 6.

2. Problem Statement and Formulation

Given a bounded domain $D \subset \mathbb{R}^2$, we seek a function $u : \mathbb{R}^2 \setminus \overline{D} \to \mathbb{C}$ which satisfies the Helmholtz equation

$$\Delta u + k^2 u = 0$$

and assumes the boundary values $g : \Gamma \to \mathbb{C}$ on the boundary $\Gamma = \partial D$. The wave number $k \in \mathbb{C}$ is chosen so that $\mathrm{Im}(k) \geq 0$. For uniqueness, the boundary value problem must be completed with an asymptotic boundary condition describing the behavior of the solution at infinity. The proper boundary condition in case of the Helmholtz equation is the *Sommerfeld radiation condition*

$$\frac{\partial u}{\partial r} - iku = o(r^{-\frac{1}{2}}) \quad \text{uniformly as} \quad r \to \infty. \tag{1}$$

Physically, (1) specifies the solution to be an outgoing wave. For the numerical treatment of this problem, we truncate the exterior domain by introducing an artificial boundary Γ_R consisting of a circle of radius R large enough to contain D in its interior (cf. Figure 1). We will find a numerical solution on the truncated domain bounded by Γ and Γ_R which we denote by Ω.

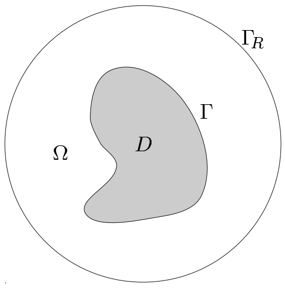

Fig. 1. The truncated domain Ω bounded externally by the circle Γ_R and internally by $\Gamma = \partial D$

On Γ_R, we impose the exact radiation boundary condition

$$\frac{\partial u}{\partial r} = M_k u, \quad |x| = R. \tag{2}$$

The mapping M_k is known as the Dirichlet-to-Neumann (DtN) mapping since it maps the Dirichlet data of a solution to the exterior Helmholtz problem with repect to the exterior of Γ_R to the correponding Neumann data. For the case of a circular artificial boundary, the DtN mapping has the explicit form (cf. Masmoudi [20] or Keller and Givoli [16])

$$M_k u = \frac{k}{2\pi} \sum_{n \in \mathbb{Z}} \frac{H_{|n|}^{(1)'}(kR)}{H_{|n|}^{(1)}(kR)} \int_0^{2\pi} u(R, \varphi) e^{in(\vartheta - \varphi)} \, d\varphi \tag{3}$$

in which $H_n^{(1)}$ is the first-kind Hankel function of order n. The DtN boundary condition given by (2) is an exact radiation condition in the sense that the solution of the problem posed on the truncated domain Ω is the restriction to Ω of the solution of the exterior problem satisfying (1). In summary, the problem we will solve numerically is

$$\begin{cases} \Delta u + k^2 u = 0 & \text{in } \Omega \\ u = g & \text{on } \Gamma \\ \dfrac{\partial u}{\partial r} = M_k u & \text{on } \Gamma_R. \end{cases} \tag{4}$$

We next formulate (4) as a variational problem in order to discretize it using the finite element method. To this end, we introduce the trial space $\mathcal{S}$ and weighting space $\mathcal{V}$ as

$$\begin{aligned}\mathcal{S} &:= \{u \in H^1(\Omega) \ : \ u_{|\Gamma} = g\}\\ \mathcal{V} &:= \{v \in H^1(\Omega) \ : \ v_{|\Gamma} = 0\},\end{aligned}$$

where $H^1(\Omega)$ is the usual Sobolev space and the boundary data is understood in the sense of the trace operator. With these definitions, the usual multiplication of the differential equation by a smooth function followed by integration by parts leads to the variational formulation:

$$\text{(5)} \qquad \textit{Find } u \in \mathcal{S} \textit{ such that} \quad a(u,v) = 0 \quad \forall v \in \mathcal{V}.$$

The sesquilinear form $a(\cdot,\cdot) : H^1(\Omega) \times H^1(\Omega) \to \mathbb{C}$ is defined as

$$a(u,v) := \int_\Omega (\nabla u \cdot \nabla \overline{v} - k^2 u \overline{v}) dx - \int_{\Gamma_R} \overline{v} M_k u \, ds,$$

where $\overline{v}$ denotes the complex conjugate of v. We note that, while the first term in the sesquilinear form is self-adjoint, the boundary integral term is only 'symmetric'. More precisely, if $\langle \cdot,\cdot \rangle_{\Gamma_R}$ denotes the duality pairing between $H^{-\frac{1}{2}}(\Gamma_R)$ and $H^{\frac{1}{2}}(\Gamma_R)$ considered as an extension of the (complex) L^2-inner product on Γ_R, we have

$$\begin{aligned}\langle M_k \varphi, \psi \rangle_{\Gamma_R} &= \int_{\Gamma_R} \overline{\psi} M_k \varphi \, ds\\ &= R \int_0^{2\pi} \left(k \sum_n \frac{H_n^{(1)\prime}(kR)}{H_n^{(1)}(kR)} \varphi_n e^{in\vartheta} \right) \overline{\psi(\vartheta)} \, d\vartheta\\ &= R \int_0^{2\pi} \left(k \sum_n \frac{H_n^{(1)\prime}(kR)}{H_n^{(1)}(kR)} \overline{\psi_n} e^{-in\vartheta'} \right) \varphi(\vartheta) \, d\vartheta'\\ &= \langle M_k \overline{\psi}, \overline{\varphi} \rangle_{\Gamma_R}.\end{aligned}$$

Because of this, the discretization matrices obtained by restricting u and v to finite dimensional subspaces of $H^1(\Omega)$ are complex-symmetric, but not Hermitian.

We now investigate some important properties of the DtN operator. In the proof of the next theorem, we will need a characterization of the dual space $H^{-p}(\Gamma_R)$ of $H^p(\Gamma_R)$ for $p \geq 0$. Since the artificial boundary Γ_R is a circle, we can write each $g \in L^2(\Gamma_R)$ as a Fourier series

$$g(\vartheta) = \sum_{n \in \mathbb{Z}} g_n e^{in\vartheta}$$

with Fourier coefficients g_n. The $H^p(\Gamma_R)$-norm of g is given by

$$\|g\|_{p,\Gamma_R} = \left\{ \sum_{n \in \mathbb{Z}} (1+n^2)^p |g_n|^2 \right\}^{1/2}.$$

A functional G on $H^p(\Gamma_R)$ belongs to the dual $H^{-p}(\Gamma_R)$ if and only if its norm

$$\|G\|_{-p,\Gamma_R} = \left\{ \sum_{n\in\mathbb{Z}} (1+n^2)^{-p} |G_n|^2 \right\}^{1/2}$$

is finite. Here G_n is the value of the functional G applied to the trigonometric monomial $\mu_n(\vartheta) := \exp(in\vartheta)$. Conversely, for every sequence of complex numbers $\{F_n\}_{n\in\mathbb{Z}}$ satisfying $\sum(1+n^2)^{-p}|F_n|^2 < \infty$, there exists an $F \in H^{-p}(\Gamma_R)$ with $F(\mu_n) = F_n,\ n \in \mathbb{Z}$.

Theorem 1. *For all non-negative integers p, the DtN operator M_k is a bounded linear operator from $H^{p+\frac{1}{2}}(\Gamma_R)$ to $H^{p-\frac{1}{2}}(\Gamma_R)$.*

Proof. We first consider the case $p = 0$. Given $g \in H^{\frac{1}{2}}(\Gamma_R)$, we must show that its image $G := M_k g$ lies in $H^{-\frac{1}{2}}(\Gamma_R)$. By the definition of M_k,

$$G(\vartheta) = k \sum_{n\in\mathbb{Z}} g_n \frac{H_n^{(1)'}(kR)}{H_n^{(1)}(kR)} e^{in\vartheta}.$$

Since

$$G_n = G(e^{in\vartheta}) = k g_n \frac{H_n^{(1)'}(kR)}{H_n^{(1)}(kR)},$$

we have

$$\begin{aligned}
\|M_k g\|^2_{\frac{1}{2},\Gamma_R} = \|G\|^2_{\frac{1}{2},\Gamma_R} &= \sum_n \frac{|G_n|^2}{(1+n^2)^{\frac{1}{2}}} \\
&= |k|^2 \sum_n \left| \frac{H_n^{(1)'}(kR)}{H_n^{(1)}(kR)} \right|^2 \frac{|g_n|^2}{(1+n^2)^{\frac{1}{2}}} \\
&= |k|^2 \sum_n |g_n|^2 (1+n^2)^{\frac{1}{2}} \left| \frac{H_n^{(1)'}(kR)}{H_n^{(1)}(kR)} \right|^2 \frac{1}{1+n^2} \\
&\le C_M^2 |k|^2 \|g\|^2_{\frac{1}{2},\Gamma_R}
\end{aligned}$$

provided we can show that there exists C_M such that

$$\left| \frac{H_n^{(1)'}(kR)}{H_n^{(1)}(kR)} \right|^2 \frac{1}{1+n^2} \le C_M^2 \qquad \text{for all } n \in \mathbb{Z}.$$

To this end, we make use of the following asymptotic formula for $H_n^{(1)}$ for large index (cf. [5]),

$$H_n^{(1)}(z) = -i\sqrt{\frac{2}{n\pi}} \left(\frac{2n}{ez}\right)^n \left\{1 + \mathcal{O}\left(\frac{1}{n}\right)\right\} \text{ as } n \to \infty, \tag{6}$$

as well as the recursion formula (cf. [19])

$$H_n^{(1)'}(z) = \frac{1}{2}\left(H_{n-1}^{(1)}(z) - H_{n+1}^{(1)}(z)\right), \qquad n \ge 1. \tag{7}$$

By (7), the expression we wish to bound becomes

$$\frac{H_n^{(1)'}(kR)}{H_n^{(1)}(kR)} = \frac{1}{2}\left(\frac{H_{n-1}^{(1)}(kR)}{H_n^{(1)}(kR)} - \frac{H_{n+1}^{(1)}(kR)}{H_n^{(1)}(kR)}\right). \tag{8}$$

Using (6) in (8), we see that the first term tends to zero and the second is $\mathcal{O}(n)$ as $n \to \infty$, yielding

$$\left|\frac{H_n^{(1)'}(kR)}{H_n^{(1)}(kR)}\right|^2 \frac{1}{1+n^2} = \mathcal{O}(n^2) \cdot \frac{1}{1+n^2} = \mathcal{O}(1) \qquad \text{as } n \to \infty,$$

which insures the existence of the desired bound C_M. The same proof works also for arbitrary $m \in \mathbb{N}$. □

Theorem 1 implies continuity of the sesquilinear form:

Corollary 1. *There exists a constant $C_b > 0$ such that*

$$|a(u,v)| \le C_b \|u\|_{1,\Omega}\, \|v\|_{1,\Omega} \qquad \forall u, v \in H^1(\Omega).$$

Proof. The Cauchy-Schwarz inequality, the boundedness of M_k and the trace theorem give, successively,

$$\begin{aligned} |a(u,v)| &\le (1+k^2)\|u\|_{1,\Omega}\, \|v\|_{1,\Omega} + \|M_k u\|_{-\frac{1}{2},\Gamma_R}\, \|v\|_{\frac{1}{2},\Gamma_R} \\ &\le (1 + k^2 + C_M C_{\text{trace}})\, \|u\|_{1,\Omega}\, \|v\|_{1,\Omega} \qquad \forall u, v \in H^1(\Omega). \end{aligned}$$

□

Theorem 2. *The DtN operator belonging to the purely imaginary wave number $k = i$ is negative definite on $H^{\frac{1}{2}}(\Gamma_R)$, i.e.*

$$\langle -M_i \psi, \psi \rangle_{\Gamma_R} \ge 0 \qquad \forall \psi \in H^{\frac{1}{2}}(\Gamma_R).$$

Proof. For any $\psi \in H^{\frac{1}{2}}(\Gamma_R)$ we have

$$\langle -M_i \psi, \psi \rangle_{\Gamma_R} = -i \sum_n |\psi|^2 \frac{H_n^{(1')}(iR)}{H_n^{(1)}(iR)} = -\sum_n |\psi|^2 \frac{K_n'(R)}{K_n(R)} \ge 0,$$

where K_n is the modified Bessel function of the third kind of order n (cf. [19]). The second identity follows from

$$H_n^{(1)}(iz) = \frac{2}{\pi i} e^{\frac{n\pi i}{2}} K_n(z)$$

valid for $-\pi < \arg(z) < \frac{\pi}{2}$. The inequality follows from the fact that $K_n(R) > 0$, $K_n'(R) < 0$ for $R > 0$, which can be inferred from the integral representation

$$K_n(z) = \int_0^\infty e^{-z\cosh t} \cosh nt \, dt$$

valid for $\mathrm{Re}(z) > 0$. □

This implies, in particular, that the sesquilinear form $a_i(\cdot,\cdot)$ belonging to $k = i$ is $H^1(\Omega)$-coercive:

$$a_i(u,u) = \int_\Omega (|\nabla u|^2 + |u|^2)\, dx - \langle M_i u, u\rangle_{\Gamma_R} \geq \|u\|^2_{1,\Omega}\,.$$

Theorem 3. *For two wave numbers k_1 and k_2 with non-negative imaginary part there holds*

$$(M_{k_1} - M_{k_2})\psi \in H^{\frac{3}{2}}(\Gamma_R) \qquad \forall \psi \in H^{\frac{1}{2}}(\Gamma_R)$$

and there exists a constant $C > 0$ such that

$$\|(M_{k_1} - M_{k_2})\psi\|_{\frac{3}{2},\Gamma_R} \leq C\|\psi\|_{\frac{1}{2},\Gamma_R}$$

Proof. By definition, we have

$$\begin{aligned}\|M_{k_1}\psi - M_{k_2}\psi\|^2_{\frac{3}{2},\Gamma_R} &= \sum_n \left| k_1 \frac{H_n^{(1)'}(k_1R)}{H_n^{(1)}(k_1R)} - k_2 \frac{H_n^{(1')}(k_2R)}{H_n^{(1)}(k_2R)} \right|^2 \psi_n|^2(1+n)^{\frac{3}{2}} \\ &\leq C^2 \sum_n |\psi_n|^2(1+n^2)^{\frac{1}{2}} \\ &= C^2\|\psi\|_{\frac{1}{2},\Gamma_R}\end{aligned}$$

provided we can establish that

$$H(n) := \left| k_1 \frac{H_n^{(1)'}(k_1R)}{H_n^{(1)}(k_1R)} - k_2 \frac{H_n^{(1)'}(k_2R)}{H_n^{(1)}(k_2R)} \right| \leq C \qquad \text{for all } n$$

for some suitable C. By the recursion formula (7),

$$\begin{aligned}H(n) = \frac{1}{2}\Bigg\{ &\left(k_1 \frac{H_{n-1}^{(1)}(k_1R)}{H_n^{(1)}(k_1R)} - k_2 \frac{H_{n-1}^{(1)}(k_2R)}{H_n^{(1)}(k_2R)} \right) \\ &- \left(k_1 \frac{H_{n+1}^{(1)}(k_1R)}{H_n^{(1)}(k_1R)} - k_2 \frac{H_{n+1}^{(1)}(k_2R)}{H_n^{(1)}(k_2R)} \right) \Bigg\}.\end{aligned}$$

As in the proof of Theorem 1, the first term in parentheses is $\mathcal{O}(1/n)$. Applying the asymptotic formula (6) to the second term yields

$$\begin{aligned}&k_1 \frac{H_{n+1}^{(1)}(k_1R)}{H_n^{(1)}(k_1R)} - k_2 \frac{H_{n+1}^{(1)}(k_2R)}{H_n^{(1)}(k_2R)} \\ &= \left(\frac{n}{n+1}\right)^{\frac{1}{2}} \left(1 + \frac{1}{n}\right)^n \left(k_1 \frac{2(n+1)}{ek_1R} - k_2 \frac{2(n+1)}{ek_2R} \right) \left\{ 1 + \mathcal{O}\left(\frac{1}{n}\right) \right\} = 0\end{aligned}$$

Thus,

$$|H(n)|^2 \cdot (1+n^2) = \mathcal{O}\left(\frac{1+n^2}{n^2}\right) = \mathcal{O}(1).$$

□

Next, we consider the following auxiliary problem: given a function $\lambda \in H^{\frac{1}{2}}(\Gamma_R)$, consider the problem (P_λ) given by

$$(P_\lambda) \quad \begin{cases} \Delta u + k^2 u = f \text{ in } \Omega \\ \qquad u = g \text{ on } \Gamma \\ \dfrac{\partial u}{\partial r} - M_k u = \lambda \text{ on } \Gamma_R. \end{cases}$$

Theorem 4. *Problem (P_λ) has a unique solution. If Γ is sufficiently regular (e.g. C^1) and if, in addition, the data satisfies $f \in L^2(\Omega)$, $g \in H^{\frac{3}{2}}(\Gamma)$ and $\lambda \in H^{\frac{1}{2}}(\Gamma_R)$, then $u \in H^2(\Omega)$ and satisfies*

$$\|u\|_{2,\Omega} \le \beta \left(\|f\|_{0,\Omega} + \|g\|_{\frac{3}{2},\Gamma} + \|\lambda\|_{\frac{1}{2},\Gamma_R} \right)$$

for some $\beta > 0$.

Proof. The proof proceeds in three steps. We begin by finding a function $u_1 \in H^2(\Omega)$ which satisfies $\Delta u_1 + k^2 u_1 = f$ in Ω. No boundary conditions are imposed so that u_1 can be found e.g. by using the Fourier transform. We set

$$\lambda_1 := \frac{\partial u_1}{\partial r} - M_k u_1 \in H^{\frac{1}{2}}(\Gamma_R)$$

and define $\tilde{u}_2$ to be the solution of the problem

$$\begin{cases} \Delta \tilde{u}_2 + k^2 \tilde{u}_2 = 0 \qquad \text{in } \mathbb{R}^2 \setminus \Gamma_R \\ \left[\dfrac{\partial \tilde{u}_2}{\partial r}\right]_{\Gamma_R} = \lambda - \lambda_1, \end{cases} \tag{9}$$

where $[v]_{\Gamma_R}$ denotes the jump $v^- - v^+$ of a function v across Γ_R as one moves from the inside to the outside. We can express $\tilde{u}_2$ as the single-layer potential (cf. [8, 17])

$$\tilde{u}_2(x) := \widetilde{S}(\lambda - \lambda_1)(x) = 2 \int_{\Gamma_R} [\lambda(y) - \lambda_1(y)] \Phi(x, y)\, ds(y)$$

with density $\lambda - \lambda_1$. The function $\Phi(x, y) = i/4\, H_0^{(1)}(k|x - y|)$ is the free-space Green's function of the Helmholtz operator satisfying the Sommerfeld condition. The mapping properties of $\widetilde{S}$ assure that $\tilde{u}_2$ lies in $H^2(\mathrm{int}(\Gamma_R))$ and in $H^2_{loc}(\mathrm{ext}(\Gamma_R))$, respectively, and the usual jump conditions for the layer potentials imply that $\tilde{u}_2$ solves the problem (9). We now set $u_2 := \tilde{u}_2|_\Omega$ and verify that

$$\frac{\partial u_2}{\partial r} - M_k u_2 = \lambda - \lambda_1 \qquad \text{on } \Gamma_R.$$

To see this, note that the DtN map M_k maps $u_2|_{\Gamma_R}$ to the normal derivative on Γ_R of the solution of the exterior Dirichlet problem with data $u_2|_{\Gamma_R}$. This normal derivative is just $\partial \tilde{u}_2^+ / \partial r$, giving

$$\frac{\partial u_2}{\partial r} - M_k u_2 = \frac{\partial \tilde{u}_2^-}{\partial r} - \frac{\partial \tilde{u}_2^+}{\partial r} = \lambda - \lambda_1.$$

We now define u_3 to be the solution of

$$\begin{cases} \Delta u_3 + k^2 u_3 = 0 & \text{in } \Omega \\ u_3 = g - u_1|_\Gamma - u_2|_\Gamma & \text{on } \Gamma \\ \dfrac{\partial u_3}{\partial r} - M_k u_3 = 0 & \text{on } \Gamma_R. \end{cases} \tag{10}$$

The regularity properties of solutions of the exterior problem (10) (cf. [18, 9]) give $u_3 \in H^2(\Omega)$ and, setting $u := u_1 + u_2 + u_3$, we obtain a solution of problem (P_λ). The continuity with respect to the data follows from standard regularity theorems or from the fact that all the operators involved are bounded. Uniqueness results from the fact that the solution of the homogeneous counterpart of (P_λ) can be extended to a solution of the homogeneous exterior Dirichlet problem, implying that it must vanish identically. □

As the final step in proving existence and uniqueness for our variational formulation, we now define the following mapping :

$$\begin{aligned} \mathcal{A} : \mathcal{V} \quad &\rightarrow \quad \mathcal{V} \\ u \quad &\mapsto \quad v = \mathcal{A}u \\ \text{such that } a_i(v, \varphi) \quad &= \quad a(u, \varphi) \quad \forall \varphi \in \mathcal{V}. \end{aligned}$$

We note that this mapping is well defined since the sesquilinear form $a_i(\cdot,\cdot)$ is coercive and $a(u,\cdot)$ is a continuous linear form on $H^1(\Omega)$.

Theorem 5. *The mapping $\mathcal{A}$ has the following properties:*

1. *$\mathcal{A}$ is a bijection from $\mathcal{V}$ to itself.*
2. *$(\mathcal{A} - I)u \in H^2(\Omega) \quad \forall v \in \mathcal{V}$.*
3. *$\mathcal{A} - I$ is a bounded linear operator from $\mathcal{V}$ to $H^2(\Omega)$, i.e. $\exists \beta > 0$:*

$$\|(\mathcal{A} - I)u\|_{2,\Omega} \leq \beta \|u\|_{1,\Omega}\,.$$

Proof. We first show that $\mathcal{A}$ is injective and surjective:
Injectivity: $\mathcal{A}u = 0$ for $u \in \mathcal{V}$ means that, for all $\varphi \in \mathcal{V}$, we have

$$0 = a_i(\mathcal{A}u, \varphi) = a(u, \varphi).$$

But this means that u is a solution of the weak homogeneous exterior Dirichlet problem which implies that $u = 0$.
Surjectivity: Given $v \in \mathcal{V}$, we need to find $u \in \mathcal{V}$ such that $\mathcal{A}u = v$. Setting $w := u - v$, we have

$$\begin{aligned} v = \mathcal{A}u \Leftrightarrow a_i(v, \varphi) &= a(u, \varphi) & \forall \varphi \in V \\ \Leftrightarrow a(w, \varphi) &= a_i(v, \varphi) - a(v, \varphi) & \forall \varphi \in V. \end{aligned}$$

The last equality, written out, says that

$$a(w, \varphi) = (1 + k^2)(v, \varphi)_{0,\Omega} + \langle (M_k - M_i)v, \varphi \rangle_{\Gamma_R} \quad \forall \varphi \in \mathcal{V}.$$

But this is a weak formulation of the following problem:

$$\begin{cases} (\Delta + k^2)w = (1+k^2)v & \text{in } \Omega, \\ w = 0 & \text{on } \Gamma, \\ \dfrac{\partial w}{\partial r} - M_k w = (M_k - M_i)v & \text{on } \Gamma_R, \end{cases}$$

which is a problem of the type (P_λ) studied previously with $\lambda = (M_k - M_i)v \in H^{\frac{3}{2}}(\Gamma_R)$. For this problem, Theorem 4 assures the existence of a unique solution w. In this case the homogeneous Dirichlet boundary condition implies $w \in \mathcal{V}$ so that $u := v + w \in \mathcal{V}$ is the desired function satisfying $\mathcal{A}u = v$ and surjectivity is shown.

By the preceding, $(I - \mathcal{A})u = u - v = w$ is the solution of (P_λ). Since $v \in \mathcal{V} \subset H^1(\Omega)$, we have $v|_{\Gamma_R} \in H^{\frac{3}{2}}(\Gamma_R)$ and thus

$$\|(M_k - M_i)v|_{\Gamma_R}\|_{\frac{3}{2},\Gamma_R} \le C\|v\|_{\frac{1}{2},\Gamma_R} \le \widetilde{C}\|v\|_{1,\Omega}\,.$$

The regularity result for w now gives

$$\|w\|_{2,\Omega} \le \beta\left((1+k^2)\|v\|_{0,\Omega} + \widetilde{C}\|v\|_{1,\Omega}\right)$$

implying $w = (\mathcal{A} - I)u \in H^2(\Omega)$.

By the estimate above, we have

$$\|(\mathcal{A} - I)u\|_{2,\Omega} = \|w\|_{2,\Omega} \le \tilde{\beta}\|v\|_{1,\Omega}$$

which proves the last assertion. □

Since $\mathcal{A}$ is bounded and surjective and maps the closed subspace $\mathcal{V}$ of $H^1(\Omega)$ onto itself, $\mathcal{A}$ is open by the open mapping theorem and thus $\mathcal{A}^{-1}$ is bounded, which means that there exists an $\alpha > 0$ such that

$$\|\mathcal{A}u\|_{1,\Omega} \ge \alpha\|u\|_{1,\Omega} \quad \forall u \in \mathcal{V}.$$

In addition, we have

Corollary 2. $\forall u \in \mathcal{V}\ \exists v \in \mathcal{V}, v \neq 0 : a(u,v) \ge \alpha\|u\|_{1,\Omega}\|v\|_{1,\Omega}$.

Proof. Choose $v := \mathcal{A}u$. Then

$$a(u,v) = a_i(v,v) \ge \|v\|^2_{1,\Omega} = \|v\|_{1,\Omega}\|\mathcal{A}u\|_{1,\Omega} \ge \alpha\|u\|_{1,\Omega}\|v\|_{1,\Omega}.$$

□

This corollary also implies uniqueness of the solution to the variational problem, since if $a(u_1,v) = a(u_2,v) = 0 \quad \forall v \in H^1(\Omega)$, it supplies the existence of $v_0 \neq 0$ such that $0 = a(u_1 - u_2, v_0) \ge \alpha\|u_1 - u_2\|_{1,\Omega}\,\|v_0\|_{1,\Omega} \ge 0$, implying $u_1 = u_2$.

3. The Discrete Variational Problem

We now consider the finite dimensional version of the variational problem. To this end, we impose a triangulation on the domain Ω into elements $\{e_j\}_{j=1}^N$ of which the longest side has length h. The elements are either triangles or rectangles. We define the finite dimensional subspaces $\mathcal{S}^h \subset \mathcal{S}$ and $\mathcal{V}^h \subset \mathcal{V}$ as spaces of continuous functions which are linear on each triangle or bilinear on each rectangle, repectively. The discrete variational problem is obtained by restricting the trial and weighting functions to $\mathcal{S}^h$ and $\mathcal{V}^h$:

$$\text{(11)} \qquad \textit{Find } u_h \in \mathcal{S}^h \textit{ such that} \quad a(u_h, v_h) = 0 \quad \forall v_h \in \mathcal{V}^h.$$

Existence, uniqueness and the best approximation property of the discrete solution u_h of (11) rest on establishing the following discrete analogue of Corollary 2:

Lemma 1. *There exist $h_0 > 0$ and $\tilde{\alpha} > 0$ such that if $h \in (0, h_0]$ there exists for every $v_h \in \mathcal{V}^h$ a function $\varphi_h \in \mathcal{V}^h$ satisfying*

$$a(v_h, \varphi_h) \geq \tilde{\alpha} \|v_h\|_{1,\Omega} \|\varphi_h\|_{1,\Omega} .$$

Before proceeding with the proof of Lemma 1, we show

Lemma 2. *Given $v_h \in \mathcal{V}^h$, define $w := \mathcal{A}v_h$ and $w_h := v_h + I_h(w - v_h)$, where $I_h : \mathcal{V} \to \mathcal{V}^h$ is the interpolation operator mapping a function in $\mathcal{V}$ to its nodal interpolant in $\mathcal{V}^h$. Then*

$$\|w - w^h\|_{1,\Omega} \leq Kh\|w\|_{1,\Omega}$$

for some constant K.

Proof. Assuming the standard interpolation estimate $\|u - I_h u\|_{1,\Omega} \leq Ch\|u\|_{2,\Omega}$, $u \in H^2(\Omega)$ for the elements under consideration, we obtain from Theorem 5

$$\begin{aligned} \|w - w_h\|_{1,\Omega} &= \|w - v_h - I_h(w - v_h)\|_{1,\Omega} \\ &= \|(\mathcal{A} - I)v_h - I_h((\mathcal{A} - I)v_h)\|_{1,\Omega} \\ &\leq Ch\|(\mathcal{A} - I)v_h\|_{2,\Omega} \\ &\leq \beta Ch\|v_h\|_{1,\Omega} . \end{aligned}$$

Also, since $\mathcal{A}$ has a bounded inverse,

$$\|w\|_{1,\Omega} = \|\mathcal{A}v_h\|_{1,\Omega} \geq \alpha\|v^h\|_{1,\Omega}$$

so that

$$\|v_h\|_{1,\Omega} \leq \frac{1}{\alpha}\|w\|_{1,\Omega} .$$

Combining these two inequalities yields

$$\|w - w^h\|_{1,\Omega} \leq \frac{\beta C}{\alpha} h\|w\|_{1,\Omega} ,$$

which is the assertion with $K = \beta C/\alpha$. □

We now turn to the proof of Lemma 1.

Proof. Given $v_h \in \mathcal{V}^h$, we have already shown that, by choosing $w = \mathcal{A}v_h$, there holds

$$a(v_h, w) \geq \alpha \|v_h\|_{1,\Omega} \|w\|_{1,\Omega}$$

and that we can find w_h satisfying

$$\|w - w_h\|_{1,\Omega} \leq hK\|w\|_{1,\Omega} .$$

Thus,

$$\begin{aligned} a(v_h, w_h) &= a(v_h, w) - a(v_h, w_h - w) \\ &\geq \alpha\|v_h\|_{1,\Omega} \|w\|_{1,\Omega} - C_b\|v_h\|_{1,\Omega} \cdot Kh\|w\|_{1,\Omega} \\ &= (\alpha - C_b Kh)\|v_h\|_{1,\Omega} \|w\|_{1,\Omega} . \end{aligned}$$

Also, from

$$\|w\|_{1,\Omega} = \|w_h - (w_h - w)\|_{1,\Omega} \geq \|w_h\|_{1,\Omega} - hK\|w\|_{1,\Omega}$$

we obtain

$$\|w\|_{1,\Omega} \geq \frac{1}{1 + hK}\|w_h\|_{1,\Omega} .$$

Thus,

$$a(v_h, w_h) \geq \frac{\alpha - C_b hK}{1 + hK}\|v_h\|_{1,\Omega} \|w_h\|_{1,\Omega}$$

This proves the assertion with $\tilde{\alpha} = (\alpha - C_b hK)/(1 + hK)$ which is positive for h sufficiently small. □

Lemma 1 yields uniqueness of the discrete solution in the same manner as in the continuous case. This also implies existence, since we are now dealing with finite dimensional spaces. The best approximation property can now be established as follows. Let $u_h \in \mathcal{S}^h$ be a solution of the discrete problem. This implies

$$a(u_h - u, \varphi_h) = 0 \quad \forall \varphi_h \in \mathcal{V}^h.$$

For arbitrary $w_h \in \mathcal{S}^h$, we then have

$$a(u_h - w_h, \varphi_h) = a(u_h - u, \varphi_h) + a(u - w_h, \varphi_h) \leq 0 + C_b\|u - w_h\|_{1,\Omega} \|\varphi_h\|_{1,\Omega} .$$

Also, to $u_h - w_h \in \mathcal{V}^h$, there exists $v_h \in \mathcal{V}^h$ with

$$a(u_h - w_h, v_h) \geq \tilde{\alpha}\|u_h - w_h\|_{1,\Omega} \|v_h\|_{1,\Omega} .$$

Thus,

$$\begin{aligned} \|u - u_h\|_{1,\Omega} &= \|u - w_h\|_{1,\Omega} + \|w_h - u_h\|_{1,\Omega} \\ &\leq \|u - w_h\|_{1,\Omega} + \frac{a(u_h - w_h, v_h)}{\tilde{\alpha}\|v_h\|_{1,\Omega}} \\ &\leq \|u - w_h\|_{1,\Omega} + \frac{C_b}{\tilde{\alpha}}\|u - w_h\|_{1,\Omega} \\ &\leq (1 + \frac{C_b}{\tilde{\alpha}})\|u - w_h\|_{1,\Omega} . \end{aligned}$$

Since w_h was arbitrary in $\mathcal{S}^h$, this implies

$$\|u - u_h\|_{1,\Omega} \leq \left(1 + \frac{C_b}{\tilde{\alpha}}\right) \inf_{w_h \in \mathcal{S}^h} \|u - w_h\|_{1,\Omega} .$$

Together with the interpolation estimate, this means that our finite element approximation converges with order h in the $H^1(\Omega)$-norm.

4. A Fast Helmholtz Solver for the Annulus

In this section, we introduce a simple finite-element discretization of the exterior Helmholtz problem on an annulus centered at the origin with a Dirichlet boundary condition imposed on the inner boundary $r = R_0$ and the DtN boundary condition imposed on the outer boundary $r = R$. This corresponds to the exterior Dirichlet problem with respect to the disk of radius R_0. We discretize in polar coordinates, i.e. our trial and test functions are piecewise polynomials in the radial and angular variables r and ϑ. We give the local and global mass and stiffness matrices for bilinear rectangles as well as the matrix belonging to the discrete DtN operator with respect to these elements. The structure of the resulting discretization matrix allows the use of an FFT based algorithm leading to a fast (exterior) Helmholtz solver for the annulus.

4.1. Bilinear Rectangles

We impose a uniform rectangular grid on the the rectangle $[R_0, R] \times [0, 2\pi)$ in the $r - \vartheta$ plane consisting of rectangles of width Δr and height $\Delta\vartheta$ and sides parallel to the coordinate axes. The four Lagrangian nodal basis functions on the rectangle with corners (r_i, ϑ_j), (r_{i+1}, ϑ_j), $(r_{i+1}, \vartheta_{j+1})$ and (r_i, ϑ_{j+1}) are then given by

$$\begin{aligned}
\varphi_1(r,\vartheta) &= \frac{r_{i+1} - r}{\Delta r} \cdot \frac{\vartheta_{j+1} - \vartheta}{\Delta\vartheta} \\
\varphi_2(r,\vartheta) &= \frac{r - r_i}{\Delta r} \cdot \frac{\vartheta_{j+1} - \vartheta}{\Delta\vartheta} \\
\varphi_3(r,\vartheta) &= \frac{r - r_i}{\Delta r} \cdot \frac{\vartheta - \vartheta_j}{\Delta\vartheta} \\
\varphi_4(r,\vartheta) &= \frac{r_{i+1} - r}{\Delta r} \cdot \frac{\vartheta - \vartheta_j}{\Delta\vartheta}.
\end{aligned}$$

Figure 2 shows a typical interior node in the mesh and the four elements to which it belongs. The element stiffness matrices K^e of the inner products

$$\int_{\Omega^e} \nabla\varphi_i \cdot \nabla\varphi_j \; dxdy = \int_{\Omega^e} \left((\varphi_i)_r (\varphi_j)_r + \frac{1}{r^2} (\varphi_i)_\vartheta (\varphi_j)_\vartheta \right) r dr d\vartheta \quad i,j = 1,2,3,4$$

for a rectangular element Ω^e are given by

$$\begin{aligned}
K^e = \frac{\Delta\vartheta}{6\Delta r} r_{i+1/2} &\begin{pmatrix} 2 & -2 & -1 & 1 \\ * & 2 & 1 & -1 \\ * & * & 2 & -2 \\ * & * & * & 2 \end{pmatrix} \\
+ \frac{\log\frac{r_{i+1}}{r_i}}{\Delta r^2 \Delta\vartheta} &\begin{pmatrix} r_{i+1}^2 & -r_i r_{i+1} & r_i r_{i+1} & -r_{i+1}^2 \\ * & r_i^2 & -r_i^2 & r_i r_{i+1} \\ * & * & r_i^2 & -r_i r_{i+1} \\ * & * & * & r_{i+1}^2 \end{pmatrix} \\
+ \frac{1}{2\Delta r \Delta\vartheta} &\begin{pmatrix} r_i - 3r_{i+1} & r_i + r_{i+1} & -r_i - r_{i+1} & -r_i + 3r_{i+1} \\ * & -3r_i + r_{i+1} & 3r_i - r_{i+1} & -r_i - r_{i+1} \\ * & * & -3r_i + r_{i+1} & r_i + r_{i+1} \\ * & * & * & r_i - 3r_{i+1} \end{pmatrix}.
\end{aligned}$$

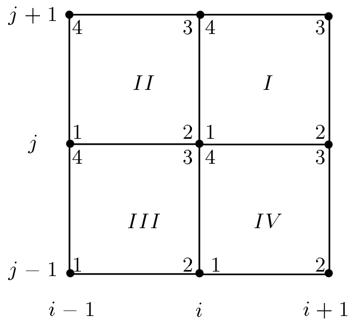

Fig. 2. Node i, j in the rectangular grid and its neighboring elements along with the local node numbering in each element.

The corresponding element mass matrices M^e of the inner products

$$\int_{\Omega^e} \varphi_i \varphi_j \; dxdy = \int_{\Omega^e} \varphi_i \varphi_j \; r dr d\vartheta \quad i, j = 1, 2, 3, 4$$

are given by

$$M^e = \frac{\Delta r \Delta\vartheta}{72} \begin{pmatrix} 8r_i + 2\Delta r & 4r_{i+1} - 2\Delta r & 2r_{i+1} - \Delta r & 4r_i + \Delta r \\ * & 8r_{i+1} - 2\Delta r & 4r_{i+1} - \Delta r & 2r_{i+1} - \Delta r \\ * & * & 8r_{i+1} - 2\Delta r & 4r_{i+1} - 2\Delta r \\ * & * & * & 8r_i + 2\Delta r \end{pmatrix}.$$

After assembly, the global stiffness matrix K for bilinear rectangles is given by

$$K = \frac{1}{\Delta\vartheta} T_1 \otimes C_1 + \frac{\Delta\vartheta}{6} T_2 \otimes C_2$$

with $n \times n$ circulant matrices

$$C_1 = \begin{bmatrix} 2 & -1 & & & -1 \\ -1 & 2 & -1 & & \\ & \ddots & \ddots & \ddots & \\ & & -1 & 2 & -1 \\ -1 & & & -1 & 2 \end{bmatrix} \text{ and } C_2 = \begin{bmatrix} 4 & 1 & & & 1 \\ 1 & 4 & 1 & & \\ & \ddots & \ddots & \ddots & \\ & & 1 & 4 & 1 \\ 1 & & & 1 & 4 \end{bmatrix}$$

and tridiagonal $m \times m$ matrices

$$T_1 = \operatorname{tridiag}(\nu_{i-1/2}, \mu_i, \nu_{i+1/2}), \qquad i = 1, \ldots, m$$

with

$$\nu_i = \frac{r_i}{\Delta r} - \frac{r_{i-1/2} r_{i+1/2}}{\Delta r} \log \frac{r_{i+1/2}}{r_{i-1/2}}$$

$$\mu_i = -\frac{2r_i}{\Delta r} + \frac{r_{i+1}^2}{\Delta r^2} \log \frac{r_{i+1}}{r_i} + \frac{r_{i-1}^2}{\Delta r^2} \log \frac{r_i}{r_{i-1}}$$

and

$$T_2 = \text{ tridiag}\left(\frac{-r_{i-1/2}}{\Delta r}, \frac{2r_i}{\Delta r}, \frac{-r_{i+1/2}}{\Delta r}\right), \qquad i = 1, \dots, m.$$

The global mass matrix M is given by

$$M = \frac{\Delta r \Delta \vartheta}{36} T_3 \otimes C_2$$

with

$$T_3 = \text{ tridiag}(r_{i-1/2}, 4r_i, r_{i+1/2}) \qquad i = 1, \dots, m.$$

The matrices above correspond to Dirichlet boundary data imposed at r_0 and r_{m+1}. Imposing a Neumann condition at the outer boundary $r = r_m$ results in modification of the m-th diagonal blocks in K and M due to a change in the (m, m) element of the tridiagonal matrices T_1, T_2 and T_3 as follows:

$$\begin{aligned} T_1 &: \mu_m \to \frac{r_{m-1}^2}{\Delta r^2} \log \frac{r_m}{r_{m-1}} - \frac{r_{m-3/2}}{\Delta r} \\ T_2 &: \frac{2r_m}{\Delta r} \to \frac{r_{m-1/2}}{\Delta r} \\ T_3 &: 4r_m \to 2r_m - \frac{\Delta r}{2}. \end{aligned}$$

A similar adjustment occurs in the case of a Neumann boundary condition at $r = r_1$.

4.2. The Discrete DtN Operator

The DtN map for the Helmholtz operator on a circle of radius R centered at the origin is given by

$$u(R, \vartheta) \mapsto u_r(R, \vartheta) =: (M_k u)(R, \vartheta)$$

in which the image $M_k g$ of a function $g \in L^2(0, 2\pi)$ is given by

$$(M_k g)(\vartheta) = \frac{k}{\pi} \sum_{\nu=0}^{\infty}{}' \frac{H_\nu^{(1)'}(kr)}{H_\nu^{(1)}(kR)} \int_0^{2\pi} g(\vartheta') \cos \nu(\vartheta - \vartheta')\, d\vartheta'.$$

The prime after the summation symbol indicates that the first term is halved. The contribution of the DtN boundary condition to the sesquilinear form of the variational formulation is thus

$$\begin{aligned} \langle M_k u, v \rangle_{\Gamma_R} &= \int_0^{2\pi} v(R, \vartheta)(M_k u(R, \vartheta) R d\vartheta \\ &= \frac{kR}{\pi} \sum_{\nu=0}^{\infty}{}' a_\nu \int_0^{2\pi} \int_0^{2\pi} v(R, \vartheta) u(R, \vartheta') \cos(\nu(\vartheta - \vartheta')) d\vartheta' d\vartheta \end{aligned}$$

where we have set $a_\nu := H_\nu^{(1)'}(kR)/H_\nu^{(1)}(kR)$. Only those nodal basis functions whose node lies on the exterior boundary will contribute to the DtN term. If those nodes are ordered last, the DtN term will result in a dense $n \times n$ block being added to the (m,m) block of the discretization matrix. If we denote by $\varphi_{i,j}$ the nodal basis function belonging to the node (r_i, ϑ_j), then the (p,q) entry in this block matrix is given by

$$\begin{aligned}
&\langle M_k \varphi_{m,p}, \varphi_{m,q} \rangle_{\Gamma_R} \\
&= \frac{kR}{\pi} {\sum_{\nu=0}^{\infty}}' a_\nu \int_{\vartheta_{p-1}}^{\vartheta_{p+1}} \int_{\vartheta_{q-1}}^{\vartheta_{q+1}} \varphi_{p,m}(R,\vartheta)\varphi_{m,q}(R,\vartheta') \cos(\nu(\vartheta - \vartheta'))d\vartheta' d\vartheta \\
&= \frac{kR}{\pi} {\sum_{\nu=0}^{\infty}}' a_\nu \frac{4(1-\cos\nu\Delta\vartheta)^2}{\Delta\vartheta^2 \nu^4} \cos(\nu(\vartheta_p - \vartheta_q)).
\end{aligned}$$

For $\nu = 0$, the expression in the summation symbol is obtained by taking the limit as $\nu \to 0$ which is $a_0 \Delta\vartheta^2$.

4.3. A Fast Helmholtz Solver

The global discretization matrix is now given by $B = K - k^2 M - \Sigma$ where the matrix

$$\Sigma = \mathbf{e}_n \mathbf{e}_n^T \otimes \sum_{\nu=0}^{N} a_\nu \Sigma_\nu$$

with matrixes $\{\Sigma_\nu\}_{\nu=0}^N$ given by

$$(\Sigma_\nu)_{j,\ell} = \cos \frac{(j-\ell)2\pi\nu}{n}$$

results from the DtN contribution. Since B consists of Kronecker products of tridiagonal and circulant matrices, the classical FFT-based fast solver (cf.[6]) can be used to solve linear systems of equations with coefficient matrix B in $\mathcal{O}(mn \log n)$ arithmetic operations.

5. A Domain Imbedding Method

Our approach is based on the work of M. Dryja and O. Widlund in the context of interior boundary value problems for self-adjoint positive operators. We first indicate how the 'Dirichlet-Neumann algorithm' developed by Bjørstadt and Widlund [23, 2, 3] can be used to obtain an imbedding algorithm for a model problem on the exterior of a disk and then generalize the idea to general domains.

5.1. The Dirichlet Neumann Algorithm for a Model Problem

We consider the exterior Helmholtz problem for a disk of radius a about the origin. Introducing an artificial boundary Γ_R at $r = R$ results in the computational domain $\{a < r < R\}$. We imbed this domain in the larger annulus $\{R_0 < r < R\}$ with some $0 < R_0 < a$ and wish to relate how an algorithm for solving the exterior problem on the larger domain can be used to recover the solution of the problem on the smaller domain. To this end, we define the sets

$$\Omega := \{(r, \vartheta) : R_0 < r < R\}$$

$$\Omega_1 := \{(r, \vartheta) : R_0 < r < a\}$$

$$\Omega_2 := \{(r, \vartheta) : a < r < R\}$$

and the interface $\Gamma = \{(r, \vartheta) : r = a\}$, so that $\Omega = \Omega_1 \cup \Gamma \cup \Omega_2$. As Ω is a rectangle in the r, ϑ plane, we can introduce a grid

$$\mathcal{G} = \mathcal{G}_{m,n} = \{(r_i, \vartheta_j) : 0 \le i \le m, \quad 0 \le j \le n-1\},$$

where $r_i = R_0 + i\Delta r, \vartheta_j = j\Delta\vartheta$, $\Delta r = (R - R_0)/m$, and $\Delta\vartheta = 2\pi/n$. By adjusting the inner radius R_0, we can arrange for Γ to coincide with a grid line (circle) $i = m_\Gamma$. This arrangement is depicted in Figure 3. The two sesquilinear

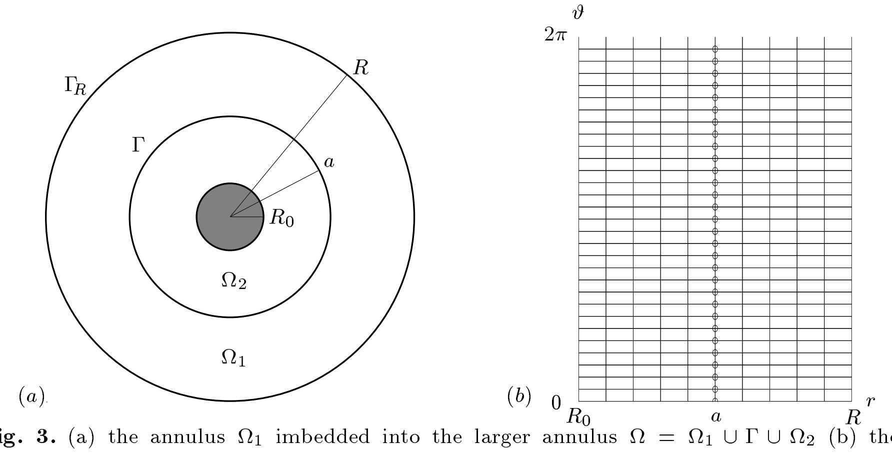

Fig. 3. (a) the annulus Ω_1 imbedded into the larger annulus $\Omega = \Omega_1 \cup \Gamma \cup \Omega_2$ (b) the corresponding uniform finite element mesh in the r,ϑ plane

linear forms

$$\begin{aligned} a_1(u,v) &= \int_{\Omega_1} (u_r \overline{v_r} + \frac{u_\vartheta \overline{v_\vartheta}}{r^2} - k^2 u \overline{v})\, r dr d\vartheta \\ a_2(u,v) &= \int_{\Omega_2} (u_r \overline{v_r} + \frac{u_\vartheta \overline{v_\vartheta}}{r^2} - k^2 u \overline{v})\, r dr d\vartheta - \int_{\Gamma_R} \overline{v} M_k u \; ds \end{aligned}$$

on appropriate function spaces correspond to the variational form of the following two boundary value problems:

$$(P_1) \begin{cases} \Delta u_1 + k^2 u_1 = 0 \text{ on } \Omega_1 \\ u_1 = 0 \text{ at } r = R_0 \\ \dfrac{\partial u_1}{\partial n} = 0 \text{ on } \Gamma \end{cases} \tag{12}$$

$$(P_2)\begin{cases} \Delta u_2 + k^2 u_2 = 0 \text{ on } \Omega_2 \\ u_2 = g \text{ on } \Gamma \\ \dfrac{\partial u_2}{\partial r} - M_k u_2 = 0 \text{ on } \Gamma_R. \end{cases} \tag{13}$$

The sum $a(\cdot,\cdot) := a_1(\cdot,\cdot) + a_2(\cdot,\cdot)$ is the sesquilinear form which belongs to the problem on the large domain Ω:

$$(P)\begin{cases} \Delta u + k^2 u = 0 \text{ on } \Omega \\ u = 0 \text{ at } r = R_0 \\ \dfrac{\partial u}{\partial n} - M_k u = 0 \text{ on } \Gamma_R. \end{cases} \tag{14}$$

We discretize problem (P) using bilinear quadrilateral elements and obtain the discretization matrix in the block form

$$B = \begin{bmatrix} A_{11} & 0 & A_{13} \\ 0 & A_{22} & A_{23} \\ A_{13}^T & A_{23}^T & A_{33} \end{bmatrix}. \tag{15}$$

with respect to the usual Lagrangian nodal basis. The partition is such that unknowns corresponding to nodes lying in Ω_1, Ω_2 and Γ have been grouped together into the first, second and third block vectors. We also define the matrices $A_{33}^{(1)}$ and $A_{33}^{(2)}$ as those contributions of A_{33} coming only from elements on the interior and exterior of Γ, respectively, so that $A_{33} = A_{33}^{(1)} + A_{33}^{(2)}$. In terms of these matrices, we can write the discretization of problems (P_1) and (P_2) as

$$\begin{bmatrix} A_{11} & A_{13} \\ A_{13}^T & A_{33}^{(1)} \end{bmatrix} \begin{bmatrix} \mathbf{u}_1 \\ \mathbf{u}_3 \end{bmatrix} = \begin{bmatrix} 0 \\ \mathbf{h} \end{bmatrix} \quad \text{and} \quad \begin{bmatrix} A_{22} & A_{23} \\ 0 & I \end{bmatrix} \begin{bmatrix} \mathbf{u}_2 \\ \mathbf{u}_3 \end{bmatrix} = \begin{bmatrix} 0 \\ \mathbf{g} \end{bmatrix},$$

where the vectors $\mathbf{g}, \mathbf{h} \in \mathbb{C}^n$ contain the Dirichlet- and Neumann data prescribed on Γ in each case. We also note that we can recover the discrete solution of (P_2) from the solution of the combined problem

$$Au := \begin{bmatrix} A_{11} & 0 & A_{13} \\ 0 & A_{22} & A_{23} \\ A_{13}^T & 0 & A_{33}^{(1)} \end{bmatrix} \begin{bmatrix} \mathbf{u}_1 \\ \mathbf{u}_2 \\ \mathbf{u}_3 \end{bmatrix} = \begin{bmatrix} 0 \\ -A_{23}\mathbf{g} \\ 0 \end{bmatrix} =: \mathbf{f} \tag{16}$$

as long as the matrix

$$\begin{bmatrix} A_{11} & A_{13} \\ A_{13}^T & A_{33}^{(1)} \end{bmatrix}$$

is non-singular, which is the case for a sufficiently fine mesh when k^2 is not an eigenvalue of the Laplacian on Ω_1 with Dirichlet data on the inner circle and Neumann data on Γ.

Following the approach introduced by Dryja, we seek the solution of (16) in the form

$$\mathbf{u} = B^{-1}\mathbf{f} + B^{-1}E\mathbf{w} \tag{17}$$

where the vector $\mathbf{w} \in \mathbb{C}^n$ is a grid function on Γ^h and $E = [0\ 0\ I_n]^T \in \mathbb{C}^{nm \times n}$ is the discrete extension operator mapping grid functions defined on Γ_h to grid functions defined on the whole grid Ω^h vanishing outside of Γ^h. This vector $\mathbf{w}$ is a solution of (16) provided that

$$\begin{aligned} 0 = A\mathbf{u} - \mathbf{f} &= A(B^{-1}\mathbf{f} + B^{-1}E\mathbf{w}) - \mathbf{f} \\ &= (B + A - B)B^{-1}\mathbf{f} + AB^{-1}E\mathbf{w} - \mathbf{f} \\ &= AB^{-1}E\mathbf{w} + (A - B)B^{-1}\mathbf{f}, \end{aligned}$$

i.e. if

$$AB^{-1}E\mathbf{w} = -(A - B)B^{-1}\mathbf{f} \tag{18}$$

holds. Since the matrices A and B agree in the first two block rows, the matrix AB^{-1} has the structure

$$AB^{-1} = \begin{bmatrix} I & 0 & 0 \\ 0 & I & 0 \\ * & * & * \end{bmatrix} \tag{19}$$

so that the first two blocks of (18) are zero. We therefore obtain an equivalent system by multiplying both sides by E^T, yielding

$$C\mathbf{w} := E^T AB^{-1}E\mathbf{w} = -E^T(A - B)B^{-1}\mathbf{f}. \tag{20}$$

The (dense) matrix C is the capacitance matrix and we will refer to (20) as the capacitance matrix equation. Once (20) has been solved, the solution $\mathbf{u}$ of (16) is easily computed by evaluating (17), which is accomplished with two applications of the fast Helmholtz solver from the previous section.

The capacitance matrix is not a simple function of the problem data, rather it must be computed at a substantial cost. If no symmetry can be exploited (cf. [11]) the cost will be n applications of the fast solver. This approach is efficient only when the exterior problem is to be solved for several right hand sides, as then the cost of the computation and factorization of C can be amortized over several problems. This situation is common for exterior Helmholtz problems resulting from plane wave scattering applications, in which the same obstacle is illuminated from many angles of incidence, each angle leading to the same exterior problem with a different right hand side,

Rather than solve (20) directly, however, we will employ an iterative method. The most powerful and versatile iterative linear system solvers are currently the family of algorithms known as *Krylov subspace methods*, of which the most well known is the Conjugate Gradient (CG) method. At the n-th step of the iteration for solving the linear system $C\mathbf{w} = \mathbf{b}$, these methods choose an approximation to $\mathbf{w}$ from the shifted Krylov space $\mathbf{w}_0 + K_n(\mathbf{r}_0, C)$ where

$$K_n(\mathbf{r}_0, C) := \operatorname{span}\{\mathbf{r}_0, C\mathbf{r}_0, \ldots, C^{n-1}\mathbf{r}_0\}$$

and $\mathbf{r}_0 = \mathbf{b} - C\mathbf{w}_0$ is the initial residual. Since the capacitance matrix C is non-Hermitian, we shall use the QMR algorithm of Freund and Nachtigal [12, 13], a very robust and efficient generalization of the CG algorithm to non-Hermitian systems which possesses many desirable mathematical properties.

In terms of computation, Krylov subspace methods require the coefficient matrix only in order to form a matrix-vector product at every step of the iteration. In case of the QMR algorithm in the implementation we use, a product with the transpose of the coefficient matrix is also necessary. Multiplication of a vector $\mathbf{w} \in \mathbb{C}^n$ by C consists of multiplying the vector $E\mathbf{w}$ by B^{-1}, an operation which can be performed by the fast Helmholtz solver, followed by multiplication with the (sparse) matrix A and, finally, multiplication of the result by the restriction matrix E^T. Due to the efficiency of the fast solver, these matrix-vector products are inexpensive to compute. Multiplication with C^T is also inexpensive, since the matrix B is (complex) symmetric and thus the fast solver can be used here as well. Multiplication with E and E^T are simply indexing operations. We also note that, even though the matrix A contains the dense $n \times n$ block due to the DtN boundary condition, multiplication by this block can be achieved efficiently using the FFT.

The convergence rate of Krylov subspace methods is governed among other things by the degree to which the spectrum of the coefficient matrix is clustered around a non-zero point in the complex plane. In the following, we will show that the spectrum of C exhibits such a clustering by showing that it is the discretization of an operator with a clustered spectrum.

To this end, we introduce the matrices

$$Q = A_{33} - A_{13}^T A_{11}^{-1} A_{13} - A_{23}^T A_{22}^{-1} A_{23} \tag{21}$$

$$Q^{(1)} = A_{33}^{(1)} - A_{13}^T A_{11}^{-1} A_{13} \tag{22}$$

$$Q^{(2)} = A_{33}^{(2)} - A_{23}^T A_{22}^{-1} A_{23} \tag{23}$$

which are the Schur complements of the matrix A and the two matrices

$$\begin{bmatrix} A_{11} & A_{13} \\ A_{13}^T & A_{33}^{(1)} \end{bmatrix} \text{ and } \begin{bmatrix} A_{22} & A_{23} \\ A_{23}^T & A_{33}^{(2)} \end{bmatrix},$$

respectively, with regard to the unknowns on Γ^h. We note that $Q = Q^{(1)} + Q^{(2)}$. One easily verifies the following relation:

$$\begin{bmatrix} A_{11} & A_{13} \\ A_{13}^T & A_{33}^{(1)} \end{bmatrix} \begin{bmatrix} A_{11} & A_{13} \\ 0 & I \end{bmatrix}^{-1} \begin{bmatrix} 0 \\ \mathbf{g} \end{bmatrix} = \begin{bmatrix} 0 \\ Q^{(1)}\mathbf{g} \end{bmatrix}. \tag{24}$$

The matrix on the left is the discrete analog of the operator belonging to the interior problem with a Neumann condition on Γ. The second matrix in (24) is the inverse of the discretization matrix of the same problem with Dirichlet data imposed on Γ. Thus, equation (24) states that the matrix $Q^{(1)}$ maps the Dirichlet data $\mathbf{g}$ into the Neumann data $Q^{(1)}\mathbf{g}$ for the interior problem. The corresponding relation for $Q^{(2)}$ and the exterior problem is

$$\begin{bmatrix} A_{22} & A_{23} \\ A_{23}^T & A_{33}^{(2)} \end{bmatrix} \begin{bmatrix} A_{22} & A_{23} \\ 0 & I \end{bmatrix}^{-1} \begin{bmatrix} 0 \\ \mathbf{g} \end{bmatrix} = \begin{bmatrix} 0 \\ Q^{(2)}\mathbf{g} \end{bmatrix}. \tag{25}$$

In this case, however, the Neumann data is given by $-Q^{(2)}\mathbf{g}$ since the normal vector then points in the opposite direction. Thus, the Schur complements $Q^{(1)}$ and $-Q^{(2)}$ are discrete interior and exterior DtN maps with respect to the boundary Γ and the problems (P_1) and (P_2).

We now relate the matrices $Q^{(1)}$ and $Q^{(2)}$ to the capacitance matrix C.

Lemma 3. *The capacitance matrix $C = E^T AB^{-1}E$ has the representation*

$$C = Q^{(1)}Q^{-1} = (I + Q^{(2)}(Q^{(1)})^{-1})^{-1}.$$

Proof. If $\mathbf{w} \in \mathbb{C}^n$ is an arbitrary vector, then $E\mathbf{w} = [0\ 0\ \mathbf{w}]^T \in \mathbb{C}^{mn}$. Letting $\mathbf{x} := B^{-1}E\mathbf{w}$ for $\mathbf{x} = [\mathbf{x}_1\ \mathbf{x}_2\ \mathbf{x}_3]^T$ gives $B\mathbf{x} = E\mathbf{w}$ which, written out, yields the block equations

$$\begin{aligned} A_{11}\mathbf{x}_1 \qquad\qquad &+A_{13}\mathbf{x}_3 &= 0\\ A_{22}\mathbf{x}_2&+A_{23}\mathbf{x}_3 &= 0\\ A_{13}^T\mathbf{x}_1+A_{23}^T\mathbf{x}_2&+A_{33}\mathbf{x}_3 &= \mathbf{w}. \end{aligned} \tag{26}$$

Since the diagonal blocks are non-singular, we obtain by block elimination $Q\mathbf{x}_3 = \mathbf{w}$ as well as $\mathbf{x}_2 = -A_{22}^{-1}A_{23}\mathbf{x}_3$ and hence

$$AB^{-1}E\mathbf{w} = A\mathbf{x} = \begin{bmatrix} A_{11} & 0 & A_{13}\\ 0 & A_{22} & A_{23}\\ A_{13}^T & 0 & A_{33}^{(1)} \end{bmatrix} \begin{bmatrix} \mathbf{x}_1\\ \mathbf{x}_2\\ \mathbf{x}_3 \end{bmatrix} = \begin{bmatrix} A_{11}\mathbf{x}_1 + A_{13}\mathbf{x}_3\\ A_{22}\mathbf{x}_2 + A_{23}\mathbf{x}_3\\ A_{13}^T\mathbf{x}_1 + A_{33}^{(1)}\mathbf{x}_3 \end{bmatrix}.$$

The first two blocks vanish by (19) and for the third block we obtain

$$\begin{aligned} A_{13}^T\mathbf{x}_1 + A_{33}^{(1)}\mathbf{x}_3 &= A_{13}^T\mathbf{x}_1 + A_{23}^T\mathbf{x}_2 + A_{33}\mathbf{x}_3 - A_{23}^T\mathbf{x}_2 - A_{33}^{(2)}\mathbf{x}_3\\ &= \mathbf{w} - A_{33}^{(2)}\mathbf{x}_3 - A_{23}^T(-A_{22}^{-1}A_{23}\mathbf{x}_3)\\ &= \mathbf{w} - Q^{(2)}\mathbf{x}_3\\ &= \mathbf{w} - Q^{(2)}Q^{-1}\mathbf{w}\\ &= (I - Q^{(2)}Q^{-1})\mathbf{w} = Q^{(1)}Q^{-1}\mathbf{w}. \end{aligned}$$

The last identity follows by factoring out Q^{-1} and using $Q = Q^{(1)} + Q^{(2)}$. □

We can obtain a representation of the continuous DtN maps with the help of the classical integral operators S, K, K^* and T which occur in the method of integral equations cf. [8, 11] for solving the Helmholtz equation. These operators are defined by

$$\begin{aligned} (K\varphi)(x) &:= 2\int_\Gamma \frac{\partial\Phi(x,y)}{\partial n(y)}\psi(y)\, ds_y, \qquad x \in \Gamma\\ (K^*\varphi)(x) &:= 2\int_\Gamma \frac{\partial\Phi(x,y)}{\partial n(x)}\varphi(y)\, ds_y, \qquad x \in \Gamma.\\ (S\varphi)(x) &:= 2\int_\Gamma \Phi(x,y)\varphi(y)\, ds_y, \qquad x \in \Gamma\\ (T\varphi)(x) &:= 2\frac{\partial}{\partial n(x)}\int_\Gamma \frac{\partial\Phi(x,y)}{\partial n(y)}\varphi(y)\, ds_y, \qquad x \in \Gamma \end{aligned}$$

where $\Phi(x,y) = H_0^{(1)}(k|x-y|)$ is the free-space Green's function of the Helmholtz operator which satisfies the Sommerfeld condition. For simplicity we set the internal radius R_0 of the imbedding annulus to zero, so that the domain Ω_1 becomes the entire disk of radius a about the origin. When $R_0 > 0$, as it will be for numerical computations which rely on the fast Helmholtz solver on an annulus, the kernels of the integral operators are replaced by a modified Green's function, i.e. the Green's function with respect to the exterior or the disk of radius R_0. The resulting modified integral operators have the same properties for our purposes, in particular, the boundary value problems with respect to Γ are uniquely solvable in terms of layer potentials resulting from the modified kernels. The modified operators also remain compact. For details on these modified and unmodified operators and their mapping properties see [11] and the references therein.

The solution of the interior Dirichlet problem with data g on Γ can be obtained as the double-layer potential

$$u_1(x) = (\widetilde{K}\varphi)(x) = \int_\Gamma \frac{\partial \Phi(x,y)}{\partial n(y)} \varphi(y)\, ds_y, \quad x \in \Omega_1$$

provided the density φ satisfies the integral equation $(I - K)\varphi = -2g$ on Γ. We also assume for the following that k^2 is not an eigenvalue of the Laplacian for either the interior Dirichlet or Neumann problems. The interior DtN map is obtained by computing the normal derivative of u_1 on Γ, which gives

$$\frac{\partial u_1}{\partial n} = \frac{1}{2}(T\varphi)(x) = -T(I-K)^{-1} g,$$

i.e. the interior DtN map, which we denote by $Q^{(-)}$, has the representation $Q^{(-)} = -T(I-K)^{-1}$. Another representation of the interior DtN map is obtained by evaluating the solution of the interior Neumann problem on Γ. The interior Neumann problem can be found as the single layer potential

$$v_1(x) = (\widetilde{S}\psi)(x) = \int_\Gamma \Phi(x,y)\psi(y)\, ds_y, \quad x \in \Gamma$$

subject to $(I + K^*)\psi = 2h$ on Γ. Thus, we have on Γ

$$v_1(x) = \int_\Gamma \Phi(x,y)\psi(y) ds_y = \frac{1}{2} S\psi(x) = S(I+K^*)^{-1} h.$$

Thus, inverting gives $Q^{(-)} = (I + K^*)S^{-1}$.

Two further representations of the interior DtN map are obtained using the representation theorem for solutions u of the interior Dirichlet and Neumann problems on Ω_1, which states that

$$\int_\Gamma \left\{ u(y)\frac{\partial \Phi(x,y)}{\partial n(y)} - \frac{\partial u}{\partial n(y)}\Phi(x,y) \right\} ds_y = \begin{cases} -u(x) & x \in \Omega_1 \\ 0 & x \in \mathbb{R}^2 \setminus \overline{\Omega_1} \end{cases}$$

Taking the limits of the values and normal derivative of this identity on Γ and using the jump relations leads to two more integral equations on Γ for the value and normal derivative of the solution:

$$(-I + K)u - S\frac{\partial u}{\partial n} = -2u \tag{27}$$

$$Tu - (I + K^*)\frac{\partial u}{\partial n} = -2\frac{\partial u}{\partial n}. \tag{28}$$

Solving each of these for the normal derivative gives

$$Q^- = S^{-1}(I - K) = (-I + K^*)T.$$

In a completely analogous way, one finds the corresponding four representations of the *exterior* DtN mapping Q^+ to be

$$Q^+ = (K^* - I)S^{-1} = T(K + I)^{-1} = S^{-1}(K - I) = (K^* + I)^{-1}T.$$

In summary, $Q^{(1)}$ is the discrete analog of Q^- and $Q^{(2)}$ that of $-Q^+$. We now choose two convenient representations for the interior and exterior DtN mappings out of the four previously derived:

$$Q^+ = (-I + K^*)S^{-1}, \qquad Q^- = (I + K^*)S^{-1},$$

yielding a continuous analog of $C = (I + Q^{(2)}(Q^{(1)})^{-1})^{-1}$ to be

$$\begin{aligned}(I - Q^+(Q^-)^{-1})^{-1} &= \left[I - (-I + K^*)(I + K^*)^{-1}\right]^{-1} \\ &= \left[(I + K^* + I - K^*)(I + K^*)^{-1}\right]^{-1} \\ &= \frac{1}{2}(I + K^*).\end{aligned}$$

The operator K^* is compact for smooth curves and data and hence its spectrum is clustered about the origin. Therefore, that of $\frac{1}{2}(I + K^*)$ will lie clustered about $\frac{1}{2}$ in the complex plane. Since C is a discrete analog of this operator, we expect its eigenvalues to approach this distribution as the discretization is refined. This indicates that Krylov subspace methods will converge quickly when used to solve the capacitance matrix equation. We have carried out numerical calculations which support these formal considerations.

5.2. The Inexact Dirichlet-Neumann Algorithm for General Domains

For a non-circular obstacle, we select an annulus $\{R_0 < r < R\}$ which contains the boundary curve Γ of the problem domain and impose a uniform rectangular grid on this annulus in the r, ϑ plane. We choose the inner radius R_0 to be positive since we then need not discretize the origin, resulting in a faster fast Helmholtz solver than had we discretized the whole disk $\{r < R\}$. Next, we modify the rectangular grid locally near Γ so that vertices in the vicinity of the Γ are moved onto Γ. The rectangles containing moved vertices are then split into two triangles along the shorter diagonal. This results in a mesh consisting mostly of uniform rectangles and a few triangles in the vicinity of Γ. Also, since nodes were only moved, there remains a one to one correspondence between the nodes of the original, uniform mesh and those of the modified mesh.

The algorithm we use to generate the locally fitted mesh from the initial uniform mesh is due to Bespalov et al. [1] and proceeds as follows :

Algorithm 5.2.1. *1. Trace the boundary curve Γ and successively collect each edge and node crossed by Γ in an edge/node list.*

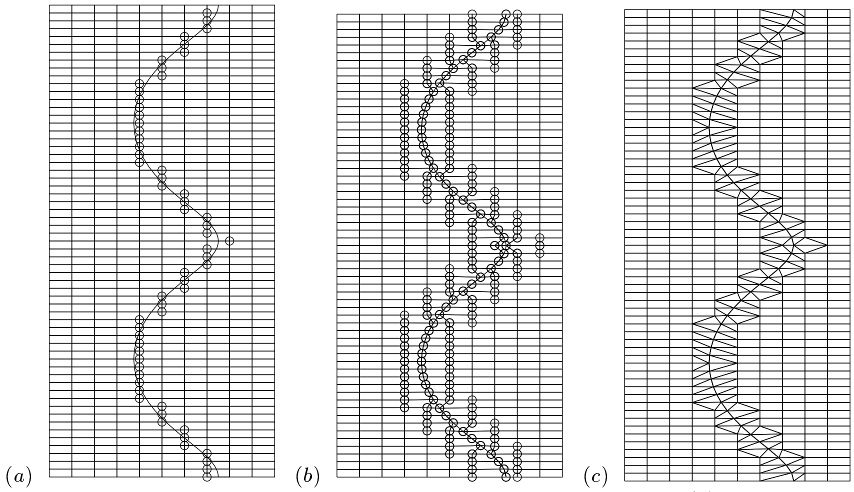

Fig. 4. The grid modification algorithm in the r,ϑ plane for an ellipse: (a) : identification of the nodes to be moved (b) : the grid with the moved boundary nodes and the nodes whose equations are affected by the grid modification (c) : the modified grid.

2. *Traverse the edge/node list and select from it a sequence of boundary nodes to be modified later. If we assume that the j-th edge/node of the list has been processed, we consider the $j+1$-st edge/node. If this is a node, then it is inserted into the sequence of boundary nodes unless it has already been inserted previously. In case of an edge, then whichever of its two end points is closer to Γ and is not already contained in the sequence is inserted unless either of its two endpoints are equal to the last inserted node. In that case no nodes are inserted for this edge.*
3. *Traverse the sequence of boundary nodes and move each one to the closest point on Γ. The sequence of moved points now constitutes the discrete boundary Γ^h.*
4. *Split each rectangle of the uniform mesh of which at least one node has moved into two triangles. If one of the diagonals of the modified rectangle belongs to the boundary Γ^h, then we divide along this diagonal, otherwise along the shorter diagonal.*

The various stages of the algorithm for the case of an ellipse are depicted in Figure 4. The curve winding through the grid is the boundary of the ellipse in polar coordinates. Figure 5 shows the resulting modified grid in the x,y plane.

When we split the unknowns into exterior, interior and boundary unknowns as in the case of the two annuli, then the resulting matrices A and B still have the same block structure as in (15) and (16), but now the matrix B is the discrete operator belonging to the annulus based on the modified mesh and hence systems with coefficient matrix B can no longer be solved with the fast Helmholtz solver. If we compare the matrix B with the matrix $\tilde{B}$ belonging to the regular mesh, however, we note that B and $\tilde{B}$ differ only in a few rows. More precisely, let us denote by $\mathcal{G}_1$ the set of interior nodes contained only in rectangles which were unaffected by the grid modification and by $\mathcal{G}_{1'}$ the remaining interior nodes.

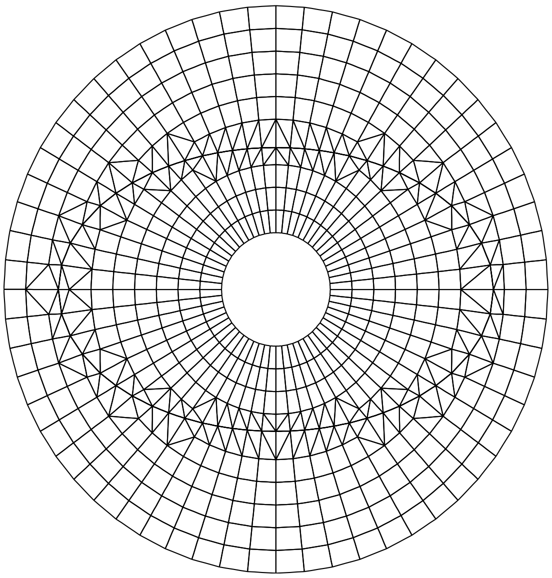

Fig. 5. The modified grid in the x,y plane

Similarly, we partition the exterior nodes into $\mathcal{G}_2$ and $\mathcal{G}_{2'}$. Denoting the set of boundary nodes by $\mathcal{G}_3$, the complete modified grid is the union of these five sets and the matrices A, B and $\tilde{B}$ have the block forms

$$A = \begin{bmatrix} A_{11} & A_{11'} & 0 & 0 & 0 \\ A_{11'}^T & A_{1'1'} & 0 & 0 & A_{1'3} \\ 0 & 0 & A_{2'2'} & A_{2'2} & A_{2'3} \\ 0 & 0 & A_{2'2}^T & A_{22} & 0 \\ 0 & A_{1'3}^T & 0 & 0 & A_{33}^{(1)} \end{bmatrix},$$

$$B = \begin{bmatrix} A_{11} & A_{11'} & 0 & 0 & 0 \\ A_{11'}^T & A_{1'1'} & 0 & 0 & A_{1'3} \\ 0 & 0 & A_{2'2'} & A_{2'2} & A_{2'3} \\ 0 & 0 & A_{2'2}^T & A_{22} & 0 \\ 0 & A_{1'3}^T & A_{2'3}^T & 0 & A_{33} \end{bmatrix}$$

and

$$\tilde{B} = \begin{bmatrix} A_{11} & A_{11'} & 0 & 0 & 0 \\ A_{11'}^T & \tilde{A}_{1'1'} & 0 & 0 & \tilde{A}_{1'3} \\ 0 & 0 & \tilde{A}_{2'2'} & A_{2'2} & \tilde{A}_{2'3} \\ 0 & 0 & A_{2'2}^T & A_{22} & 0 \\ 0 & \tilde{A}_{1'3}^T & \tilde{A}_{2'3} & 0 & \tilde{A}_{33} \end{bmatrix}.$$

We see that B and $\tilde{B}$ differ in the block rows corresponding to $\mathcal{G}_1'$, $\mathcal{G}_2'$ and $\mathcal{G}_3$. If we look for a solution $\mathbf{u}$ of the combined problem $A\mathbf{u} = \mathbf{f}$ in the form

$$\mathbf{u} = \tilde{B}^{-1}\mathbf{f} + \tilde{B}^{-1}\tilde{E}\mathbf{w}$$

with

$$\mathbf{f} = \begin{bmatrix} 0 \\ 0 \\ -A_{2'3}\mathbf{g} \\ 0 \\ 0 \end{bmatrix} \qquad \text{and} \qquad \tilde{E} = \begin{bmatrix} 0 \\ I \\ I \\ 0 \\ I \end{bmatrix} \in \mathbb{C}^{mn \times \tilde{n}}, \quad \tilde{n} = |\mathcal{G}_{1'} \cup \mathcal{G}_{2'} \cup \mathcal{G}_3|,$$

each I denoting the identity matrix of its block, then, as in the case of the two annuli, $\mathbf{u}$ solves the system $A\mathbf{u} = \mathbf{f}$ provided $\mathbf{w}$ solves the capacitance matrix equation

$$\tilde{C}\mathbf{w} := \tilde{E}^T A \tilde{B}^{-1} \tilde{E} = -(A - \tilde{B})\tilde{B}^{-1}\mathbf{f}. \tag{29}$$

Now the multiplication of a vector by the capacitance matrix equation can once again be performed using the fast Helmholtz solver. The dimension of the capacitance matrix remains proportional to the number of unknowns on the boundary Γ.

6. Numerical Results

In this section we give some representative results from an implementation of the algorithm previously described. All computations were carried out on an IBM RS/6000 model 370 workstation which has a peak speed of 125 Mflops. The QMR implementation used is that of Freund and Nachtigal version 1.2.

6.1. Computations with a Model Problem

We first apply the imbedding algorithm to a model problem for which we don't have to deal with the geometry of Γ and for which we know an exact solution: the plane-wave scattering problem for the exterior of a disk of radius a with the circular artificial boundary at $R = 1$. For this problem, the Dirichlet data on Γ is given by $u(a, \vartheta) = -\exp(ika\cos(\varphi - \vartheta))$ where φ is the angle of incidence of the plane wave. We imbed the annular computational domain $\{a < r < R\}$ into the larger annulus $\{R_0 < r < R\}$ for an $R_0 < a$. Table 1 shows the iteration counts for three different wave numbers and several grids. We have set $R_0 = 0.25$, $a = 0.5$, $R = 1$ and have chosen k so that there are $1/8$, 1 and 8 wavelengths between a and R. In all cases the angular resolution was chosen to be six times that of the radial direction. The stopping criterion for the iteration was a reduction of the initial residual by 10^{-8}. We observe that, as soon as the waves are resolved, which occurs for roughly five to ten grid points per wavelength, the iteration count does indeed remain constant. In the case of eight waves it actually decreases somewhat.

Comparison of the residual curves shows these to be nearly identical across grids of different resolution in all three cases. For this simple test problem, it was feasible to calculate the eigenvalues of the capacitance matrix C numerically, and these were indeed clustered around $1/2$. This cluster, however, grows in size with the wave number k, which is reflected in the increase in iteration counts as k grows.

1/8 wave ($k = \pi/2$)			1 wave ($k = 4\pi$)			8 waves ($k = 32\pi$)		
grid size	$\Delta r/\lambda$	it's	grid size	$\Delta r/\lambda$	it's	grid size	$\Delta r/\lambda$	it's
15×90	1/80	5	15×90	1/10	12			
30×180	1/160	5	30×180	1/20	12			
60×360	1/320	5	60×360	1/40	12	60×360	1/5	63
			120×720	1/80	12	120×720	1/10	60
			240×1440	1/160	12	240×1440	1/20	57

Table 1. Iteration counts for the iterative imbedding method applied to the two annular domains

6.2. Computations with general domains

As an example of how the algorithm performs for a more general (non-circular) domain, we give the results of applying the inexact Dirichlet-Neumann algorithm described in the previous section to solve the exterior Helmholtz problem with respect to an ellipse with semi-axes $a = 0.8$ and $b = 0.5$. The inner radius of the imbedding annulus is chosen as $R_0 = 0.2$. Table 2 shows the cpu times and the iteration counts for various grid sizes and wave numbers as well as two angles of incidence.

ellipse: $a = 0.8$, $b = 0.5$, $R_0 = 0.2$, $R = 1$				
$\vartheta_{inc} = 0^o$				
grid size	$k = 2\pi$	$k = 4\pi$	$k = 8\pi$	$k = 16\pi$
10×60	0.4 (25)	0.5 (27)	0.8 (43)	2.8 (159)
20×120	1.6 (25)	1.8 (28)	2.7 (42)	4.1 (66)
40×240	6.2 (26)	6.9 (29)	10.5 (44)	15.2 (63)
80×480	26.4 (25)	30 (29)	47.5 (45)	64.4 (61)
160×960	120.3 (26)	134 (29)	208.5(45)	287.6 (62)
$\vartheta_{inc} = 45^o$				
grid size	$k = 2\pi$	$k = 4\pi$	$k = 8\pi$	$k = 16\pi$
10×60	0.5 (31)	0.7 (39)	1.1 (64)	-
20×120	1.9 (31)	2.8 (45)	3.8 (62)	7.4 (118)
40×240	7.6 (32)	11.0 (46)	15.4 (65)	25.5 (107)
80×480	35.7 (34)	51.5 (49)	70.7 (67)	107.7 (102)
160×960	148.2 (32)	231.7(50)	321.6 (69)	513.2 (110)

Table 2. Times and iteration counts for the ellipse geometry

In case of zero degree incidence, the symmetry of the problem with respect to the x-axis leads to artificially lower iteration counts. We notice basically the same behavior as in the model problem, namely that the iteration counts for one wave number remains (nearly) constant across various grid sizes as soon as the waves are resolved. We also observe the increase of the iteration count as k increases; the growth in this and other cases observed, the growth is rather mild and seems to be proportional to $\sqrt{k}$, although we have no theory to support this. The iteration counts for individual wave numbers are no longer exactly constant as the grid is refined. We attribute this to the quality of the mesh modification algorithm, in which no attention was paid to the size and shape of the triangles generated near Γ. We expect an improved mesh generator to remove these small variations. The increase in cpu time is of course due to the increased cost of each iteration, which in turn results from the growth in cost of applying the fast Helmholtz solver, which is proportional to the grid size except for a logarithmic term. This growth is can be observed in the cpu times.

7. Conclusions

We have shown how the techniques of imbedding methods combined with fast solvers may be extended to exterior problems for the Helmholtz equation by using the exact DtN boundary condition leading to fast Helmholtz solvers for annular domains. We have also shown that the Dirichlet-Neumann imbedding algorithm leads to capacitance matrices with favorable spectral distributions making them ideal candidates for Krylov subspace algorithms such as QMR for the iterative solution of the capacitance matrix equation. The numerical results support the formal considerations regarding the mesh independent convergence rates for Krylov subspace methods applied to this problem. The resulting algorithm thus retains the efficiency of similar techniques applied to interior problems for self-adjoint positive-definite elliptic boundary value problems.

Acknowledgement. The author wishes to thank Prof. Gene H. Golub for supervising the author's thesis project, out of which this paper resulted, and Prof. Robert Dutton for support and providing access to his computing environment.

References

1. A. Bespalov, Y. Kuznetsov, O. Pironneau, and M. Vallet, *Fictitious domains with separable preconditioners versus unstructured adapted meshes*, Tech. Report 1614, INRIA, February 1992.
2. P.E. Bjørstadt and O.B. Widlund, *Solving elliptic problems on regions partitioned into substructures*, Elliptic Problem Solvers II (G. Birkhoff ans A. Schoenstadt, ed.), 1984, pp. 245–255.
3. ———, *Iterative methods for the solution of elliptic problems on regions partitioned into substructures*, SIAM J. Numer. Anal. **23** (1986), no. 6, 1097–1120.
4. C. Börgers and O. B. Widlund, *On finite element domain imbedding methods*, SIAM J. Numer. Anal. **27** (1990), no. 4, 963–978.
5. J.J. Bowman, T.B.A. Senior, and P.L.E. Uslenghi, *Electromagnetic and acoustic scattering by simple shapes*, 2 ed., Hemisphere Publishing Corporation, 1987.
6. B. Buzbee, G. Golub, and C. Nielson, *On direct methods for solving Poisson's equation*, SIAM J. Numer. Analysis **7** (1970), 627–656.
7. B.L. Buzbee, F.W. Dorr, J.A. George, and G.H. Golub, *The direct solution of the discrete Poisson equation on irregular regions*, SIAM J. Numer. Anal. **8** (1974), 722–736.
8. D. Colton and R. Kress, *Integral equation methods in scattering theory*, Wiley, New York, 1983.
9. ———, *Inverse acoustic and electromagnetic scattering theory*, Applied Mathematical Sciences, vol. 93, Springer-Verlag, 1992.
10. M. Dryja, *A finite-element capacitance matrix method for the elliptic problem*, SIAM J. Numer. Anal. **20** (1983), 621.
11. O.G. Ernst, *Fast numerical solution of exterior Helmholtz problems with radiation boundary condition by imbedding*, Ph.D. thesis, Stanford University, 1994.
12. R.W. Freund and N.M. Nachtigal, *Implementation details of the coupled QMR algorithm*, Tech. Report 92.19, RIACS, 1992.
13. ———, *An implementation of the QMR method based on coupled two-term recurrences*, SIAM J. Sci. Comput. **15** (1994), no. 2, 313–337.

14. A. George, *The use of direct methods for the solution of the discrete Poisson equation on non-rectangular regions*, Tech. Report STAN-CS-70-159, Computer Science Dept., Stanford University, Stanford, CA, 1970.
15. R. W. Hockney, *POT4–A fast direct Poisson-solver for the rectangle allowing some mixed boundary conditions and internal electrodes*, Tech. report, IBM Thomas J. Watson Research Center, Yorktown Heights, NY 10598, May 1970.
16. J. B. Keller and D. Givoli, *Exact non-reflecting boundary conditions*, J. Comput. Phys. **82** (1989), 172–192.
17. A. Kirsch, *Generalized Boundary Value- and Control Problems for the Helmholtz Equation*, Habilitation thesis, Göttingen, 1984.
18. ———, *Remarks on some notions of weak solutions for the Helmholtz equation*, Appl. Anal. **14** (1992), 7–24.
19. N.N. Lebedev, *Special functions and their applications*, Dover, 1972.
20. M. Masmoudi, *Numerical solution for exterior problems*, Numer. Math. **51** (1987), 87–101.
21. W. Proskurowski and O. B. Widlund, *On the numerical solution of Helmholtz's equation by the capacitance matrix method*, Math. Comp. **30** (1976), 433–468.
22. P. N. Swarztrauber, *The methods of cyclic reduction, fourier analysis and the facr algorithm for the discrete solution of Poisson's equation on a rectangle*, SIAM Rev. **19** (1977), 490–501.
23. O.B. Widlund, *Iterative methods for elliptic problems on regions partitioned into substructures*, Proc. 6th Intern. Conf. Comput. Meth. Sci. Eng. (R. Glowinski and J.L. Lions, eds.), Elsevier Science Publishers B. V. (North Holland), 1984, pp. 33–45.

This article was processed by the author using the LaTeX style file *cljour1* from Springer-Verlag.